physica status solidi a

www.pss-a.com

applications and materials science

The Silicon Age

Guest Editors
Martin Kittler and Deren Yang

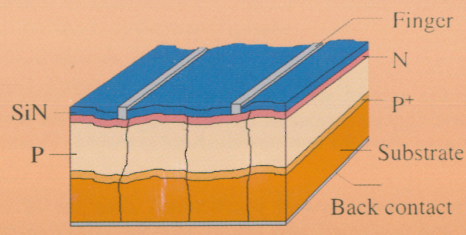

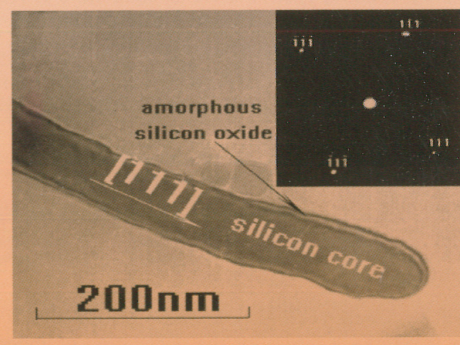

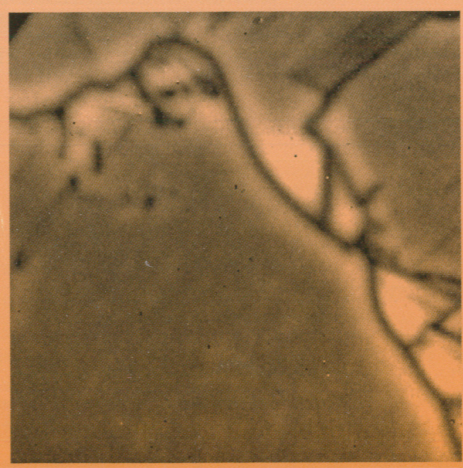

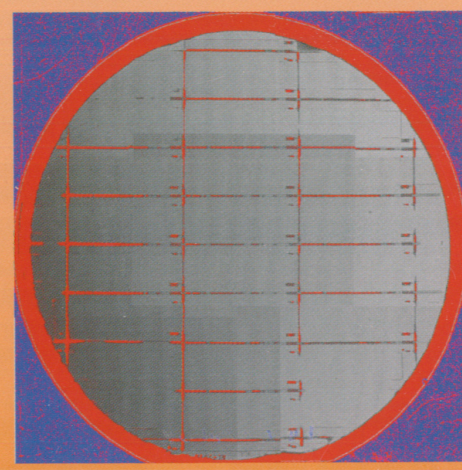

With contributions from the 2nd Sino-German Symposium,
Cottbus, Germany, 19–24 September 2005

SPECIAL ISSUE

203 • 4 • March 2006

WILEY-VCH

ISSN 0031-8965, phys. stat. sol. (a)
203, No. 4, R19–R34, 651–810 (2006)

physica status solidi a
www.pss-a.com
applications and materials science

203 · 4 (4 of 15)
March · 2006

WILEY-VCH

pss physica status solidi (a) – applications and materials science

Editor-in-Chief:	Martin Stutzmann
Managing Editor:	Stefan Hildebrandt
Editor:	Ron Schulz-Rheinländer
Production Editors:	Heike Höpcke, Irina Juschak, Dietmar Reichelt
Editorial Assistance:	Julia Hübner, Margit Schütz, Kathrin Telle
Editorial Office:	*pss* physica status solidi Bühringstr. 10, 13086 Berlin, Germany Telephone: +49 (0) 30/47 03 13 31, Fax +49 (0) 30/47 03 13 34 e-mail: pss@wiley-vch.de
Publishers:	WILEY-VCH Verlag GmbH & Co. KGaA, Weinheim
Postal Address:	Bühringstr. 10, 13086 Berlin, Germany
Editorial Director:	Alexander Grossmann
Ordering:	Subscription Service, WILEY-VCH Verlag GmbH & Co. KGaA Postfach 10 11 61, 69451 Weinheim, Germany Telephone +49 (0) 62 01/60 64 00, Fax +49 (0) 62 01/60 61 84 e-mail: subservice@wiley-vch.de or through a bookseller
Printing House:	Druckhaus Thomas Müntzer GmbH, Bad Langensalza, Germany Printed on chlorine- and acid free paper.

physics status solidi (a) – applications and materials science is published fifteen times per year by WILEY-VCH Verlag GmbH & Co. KGaA.

Annual subscription rates 2006 for pss (a) and pss (c) *or* pss (b) and pss (c):

		Institutional*
Europe	Euro	5058/4598
Switzerland	SFr	8028/7298
All other areas	US$	6598/5998

Annual subscription rates 2006 for pss (a), pss (b) and pss (c):

		Institutional*
Europe	Euro	10116/9196
Switzerland	SFr	16056/14596
All other areas	US$	13196/11996

Please contact journals customer service for information on the benefits of an **Enhanced Access Licence.**

pss (a) and/or pss (b) subscriptions: Now including pss (c) – conferences and critical reviews
* print **and** electronic/print only **or** electronic only

Personal rates are available on request.
Postage and handling charges included. All WILEY-VCH prices are subject to local VAT/sales tax.
Prices are subject to change.

For our American customers:
physica status solidi (a) – applications and materials science (ISSN 0031-8965, CODEN PSSABA) is published fifteen times per year by WILEY-VCH Verlag GmbH & Co. KGaA, Boschstr. 12, 69469 Weinheim, Germany. Periodicals postage paid at Jamaica, NY 11431. Air freight and mailing in the USA by Publications Expediting Service Inc., 200 Meacham Ave., Elmont, NY 11003. US Postmaster: send address changes to: physica status solidi (a), c/o WILEY-VCH, 111 River Street, Hoboken, NJ 07030.

Contents

Rapid Research Letters

Continuous-wave and tunable laser operation of $Tm:LuVO_4$ near 1.9 μm under Ti:sapphire and diode laser pumping
X. Mateos, J. Liu, H. Zhang, J. Wang, M. Jiang, U. Griebner, and V. Petrov R19–R21

Decrease of dielectric loss in $CaCu_3Ti_4O_{12}$ ceramics by La doping
Lixin Feng, Xiaoming Tang, Yueyue Yan, Xuezhi Chen, Zhengkuan Jiao, and Guanghan Cao R22–R24

Threading dislocation density reduction in two-stage growth of GaN layers
V. E. Bougrov, M. A. Odnoblyudov, A. E. Romanov, T. Lang, and O. V. Konstantinov R25–R27

Annealing effects on the photoresponse of TiO_2 nanotubes
Andrei Ghicov, Hiroaki Tsuchiya, Jan M. Macak, and Patrik Schmuki R28–R30

Spatially resolved deformation studies on carbon steel employing X-rays and positron annihilation
Matz Haaks, Ingo Müller, Andreas Schoeps, and Hermann Franz R31–R33

Original Papers

Papers presented at the The Silicon Age 2nd Sino–German Symposium, Cottbus, Germany, 19–24 September 2005

Guest Editors: Martin Kittler and Deren Yang

Preface 657–658

Wafering of silicon crystals
H. J. Möller 659–669

Effects of rapid thermal processing on oxide precipitation in conventional and nitrogen-doped Czochralski silicon
Xiangyang Ma, Liming Fu, Daxi Tian, Can Cui, and Deren Yang 670–676

A contribution to oxide precipitate nucleation in nitrogen doped silicon
G. Kissinger, U. Lambert, M. Weber, F. Bittersberger, T. Müller, H. Richter, and W. von Ammon 677–684

Germanium effect on oxygen-related defects in Czochralski silicon
Deren Yang, Jiahe Chen, Hong Li, Xiangyang Ma, Daxi Tian, Liben Li, and Duanlin Que . . . 685–695

Gettering in silicon photovoltaics: current state and future perspectives
M. Seibt, A. Sattler, C. Rudolf, O. Voß, V. Kveder, and W. Schröter 696–713

R&D activities of silicon-based thin-film solar cells in China
Yuwen Zhao, Xinhua Geng, Wenjing Wang, Xudong Li, and Ying Xu 714–720

Polycrystalline silicon thin-film solar cells on various substrates
Wenjing Wang, Ying Xu, and Hui Shen. 721–731

Advanced defect and impurity diagnostics in silicon based on carrier lifetime measurements
W. Warta 732–746

Semiconductor wafer bonding
M. Reiche 747–759

Silicon-based narrow-bandgap thin-film semiconductor materials: polycrystalline SiGe prepared by reactive thermal CVD
Jianjun Zhang, Kousaku Shimizu, Ying Zhao, Xinhua Geng, and Jun-ichi Hanna 760–775

Ge-dots/Si multilayered structures fabricated by Ni-induced lateral crystallization
Y. Shi, B. Yan, L. Pu, K. J. Zhang, P. Han, R. Zhang, and Y. D. Zheng 776–780

Pressure-induced transformations of nitrogen implanted into silicon
V. D. Akhmetov, A. Misiuk, A. Barcz, and H. Richter 781–785

Involvement of iron–phosphorus complexes in iron gettering for n-type silicon
T. Mchedlidze and M. Kittler 786–791

Synthesis and Raman spectra of Si-nanowires
Z. X. Su, J. Sha, J. J. Niu, J. X. Liu, and D. R. Yang 792–801

Silicon-based light emitters
M. Kittler, M. Reiche, T. Arguirov, W. Seifert, and X. Yu 802–809

physica status solidi (a) is indexed in Cambridge Scientific Abstracts; Chemical Abstracts; GeoRef; Google Scholar; Infotrieve ArticleFinder; INIS Database; INIST PASCAL, ARTICLE@INIST; INSPEC, Physics Abstracts; ISI Index to Scientific & Technical Proceedings, Current Contents/Physical, Chemical & Earth Sciences, Science Citation Index, Web of Science; OCLC WorldCat, OCLC ArticleFirst; Scopus; VINITI.

DOI: The fastest way to find an article online is the *Digital Object Identifier* (DOI). DOIs are printed in the header of the first page of every article. On the WWW, one can find an article for example with a DOI of 10.1002/pssa.200306608 at **http://dx.doi.org/**10.1002/pssa.200306608. Please use the DOI of the article to link from your home page to the articles in Wiley Interscience. The DOI is a system for the persistent identification of documents on digital networks, see **www.doi.org.**

phys. stat. sol. (a) **203**, No. 4, 696–713 (2006) / **DOI** 10.1002/pssa.200664516

Gettering in silicon photovoltaics: current state and future perspectives

M. Seibt*, **A. Sattler****, **C. Rudolf, O. Voß, V. Kveder*****, and **W. Schröter**

IV. Physikalisches Institut, Georg-August-Universität Göttingen, Friedrich-Hund-Platz 1, 37077 Göttingen, Germany

Received 30 January 2006, accepted 14 February 2006
Published online 14 March 2006

PACS 61.72.Cc, 61.72.Ff, 61.72.Yx, 71.55.Cn, 72.40.+w, 81.05.Cy

This paper summarizes current understanding and predictive simulations of gettering processes predominantly applied in silicon photovoltaics. Special emphasis is put on various processes limiting gettering efficiency and kinetics, i.e. the mobility of interstitially dissolved metal species, the formation of the gettering layer, and the effect of immobile metal species. The latter are substitutional metal species, precipitates, complexes with defects related to non-metallic impurities, and finally the interaction with extended defects, in particular dislocations. Finally, alternative annealing schemes involving high-temperature rapid thermal processing are explored by simulations. It is shown that a processing window exists for a two-step process efficient for the removal of precipitates even under the constraints of a fixed thermal budget for phosphorus diffusion.

1 Introduction

Low-cost crystalline silicon materials are increasingly used for main-stream photovoltaic applications. Such materials contain various extended defects, e.g. grain boundaries, second phase precipitates and in particular grown-in dislocations. The latter are known to strongly affect the minority carrier lifetime and hence the solar cell efficiency, especially when decorated with metal impurities either in form of various point defect species or as metal silicide precipitates. Hence, the incorporation of gettering steps into the processing scheme is a prerequisite for the production of efficient solar cells. Metal impurities may be incorporated into solar cell silicon materials during crystal growth and also during device processing. Recent investigations of the metal impurity content of silicon solar cell materials have shown surprisingly high concentrations, e.g. 10^{14}–10^{16} cm^{-3} iron in different multicrystalline materials [1].

Metal impurity gettering is a process of semiconductor device manufacturing technology and techniques suitable for gettering are intimately linked to the device under consideration. An illustrative example is to compare the requirement of silicon microelectronics and silicon photovoltaics. Active areas of microelectronic devices are located in a thin region below the wafer surface, i.e. impurity gettering to the bulk of the wafer in order to clean the surface-near region is a suitable process so that *internal gettering* [2] is the technique of choice [3, 4]. Solar cells, however, are whole-wafer devices implying that *external gettering* techniques have to be used. In fact, phosphorus diffusion gettering (PDG) and aluminum gettering (AlG) are the gettering techniques predominantly applied in silicon photovoltaics. Both steps are not

* Corresponding author: e-mail: seibt@ph4.physik.uni-goettingen.de, Phone: +49 551 394553, Fax: +49 551 394560
** now at: Siltronic AG, P.O. Box 1140, 84479 Burghausen, Germany
*** permanent address: Inst. of Solid State Physics, Russian Academy of Science, Chernogolovka, 142432 Russia

primarily included for the sake of gettering but to produce functional parts of the device, i.e. the highly phosphorus doped emitter and the backsurface field, respectively, both for p-type silicon solar cells.

The fact that gettering has to fit in manufacturing processes and that impurities are gettered to active parts of the device, in particular the front-side emitter, imposes constraints on the thermal budget and on possible processing schemes under which gettering has to operate. It is thus advisable to develop *predictive simulation tools* [5–8] by which various processing schemes can be explored for their gettering efficiency and compatibility with solar cell production. Such a simulation tool has to describe processes like phosphorus diffusion, metal impurity diffusion, interaction with intrinsic point defects, precipitate dissolution and growth, only to mention a few. For multicrystalline materials, in addition, metal impurity interaction with extended defects like dislocations and grain boundaries is an important issue [9] because of the tremendous effect of metal decoration on the recombination activity of dislocations [10].

In this paper, quantitative experiments as well as predictive simulations will be summarized and used to review effects significantly affecting gettering efficiency and kinetics. Section 2 gives a brief introduction into the underlying physical processes of PDG and AlG, and describes an experimental approach to quantitatively follow gettering kinetics without interfering effects of sample cooling to room temperature and the complexity and uncertainty to extract total metal concentrations from electrical measurements. This section concludes with lining out the possibilities of the simulation tool used in the remainder of this work. Phenomena limiting gettering efficiency and kinetics are described in Section 3 including immobile metal impurity species, precipitates, complexes and the interaction with dislocations. Alternative schemes including *rapid thermal processing, RTP,* are discussed in Section 4 where it is shown that a suitable combination of a high temperature dissolution step and a low-temperature gettering step allows to effectively remove precipitated metal impurities under the constraints of emitter production.

2 Gettering techniques for silicon photovoltaics and their quantitative assessment

As mentioned above, silicon solar cells have to be regarded as *whole-wafer devices* which implies that gettering techniques have to be of external type. Two gettering processes are usually active during solar cell processing, i.e. phosphorus diffusion gettering (PDG), as part of the emitter diffusion in p-type solar cells, and aluminum gettering (AlG) which takes place during formation of the back-surface field. In this section, the underlying physics of these two techniques are briefly summarized. In addition, quantitative modeling and experimental verification of impurity redistribution during gettering as used in the remaining part of this paper is described.

2.1 Aluminum gettering

The underlying physics of aluminum gettering is simply the higher solubility of metal impurities in the Al:Si melt forming on the backside of silicon wafers if the temperature exceeds the eutectic temperature of the binary system Al–Si of $T_{\mathrm{eut}} = 577$ °C [11]. It can be quantified by means of the segregation coefficient S_{AlG} which is defined as the ratio of the metal concentrations in the Al:Si melt and silicon in thermodynamic equilibrium:

$$S_{\mathrm{AlG}} = \frac{c_{\mathrm{Al:Si}}^{(\mathrm{eq})}}{c_{\mathrm{Si}}^{(\mathrm{eq})}} . \tag{1}$$

In the presence of the Al:Si layer on the wafer backside, metal impurities will redistribute such that the final concentration ratio is given by Eq. (1) whereas the actual concentrations have to be calculated from the continuity equation for metal impurities:

$$\int_{\mathrm{AlSi}} c_{\mathrm{AlSi}}(x)\,\mathrm{d}x + \int_{\mathrm{Si}} c_{\mathrm{Si}}(x)\,\mathrm{d}x = \int_{\mathrm{Si}} c_{\mathrm{Si}}(x, t=0)\,\mathrm{d}x , \tag{2}$$

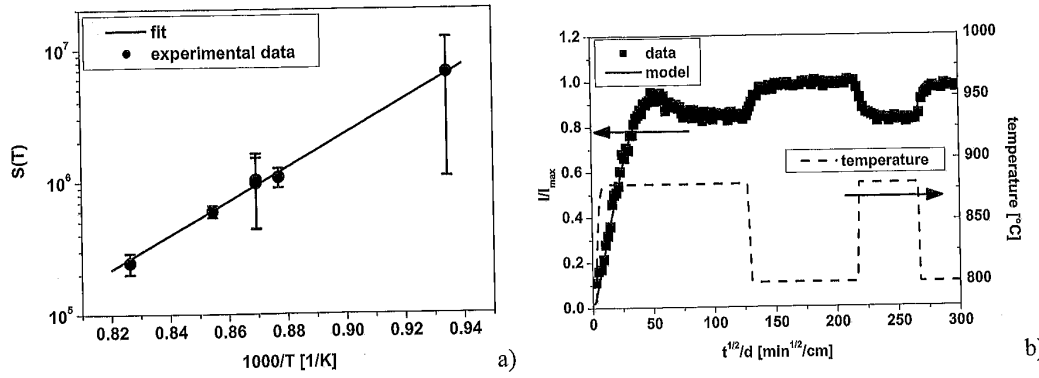

Fig. 1 (online colour at: www.pss-a.com) Aluminum gettering of cobalt in float-zone silicon. (a) Segregation coefficient $S(T)$ of cobalt in Al:Si melt as a function of temperature as measured by radiotracer technique [12, 13]. (b) Normalized intensity I/I_{max} – basically corresponding to the fraction of gettered cobalt – as a function of reduced gettering time $\sqrt{t}/d$ (d: sample thickness, t: AlG gettering time) for variable temperatures indicated on the right scale. The amount of gettered cobalt varies according to the temperature dependence of the segregation coefficient. It should be noted that cobalt atoms reversibly redistribute between the silicon and the Al-gettering layer according to the segregation coefficient shown in (a).

where the integrals have to be taken over the thickness of the Al:Si-layer and the wafer thickness as indicated. The main features of impurity segregation are (i) a temperature-dependent segregation coefficient, and (ii) the reversibility of impurity redistribution which, to first order, exclusively depends on temperature. It should be noted that the segregation coefficient as given by Eq. (1) will usually decrease with increasing temperature due to the – compared to metallic alloys – strong thermal activation of the solubility of metal impurities in silicon.

Figure 1(a) shows the segregation coefficient of cobalt in the Al:Si melt referred to float-zone silicon as a function of temperature. It has been determined by measuring *total* cobalt concentrations by means of radioactive ^{57}Co deliberately introduced into silicon and subsequently gettered to the Al:Si melt [12]. The reversibility of the redistribution between the silicon and the Al:Si melt is demonstrated by the results summarized in Fig. 1(b). It shows the normalized intensity I/I_{max} of the 6.4 keV radiation resulting from the $^{57}Co \rightarrow {}^{57}Fe$ decay as measured from the Al:Si layer *during* the gettering heat treatment (see Section 2.3 for details). The variation of the gettering temperature (dashed line, right scale) induces the reversible redistribution of the cobalt between the Al:Si gettering layer and the silicon bulk according to the segregation coefficient shown in Fig. 1(a).

2.2 Phosphorus diffusion gettering

Phosphorus diffusion gettering (PDG) comes about due to a variety of physical processes briefly described below. For more detailed discussions, the reader is referred to [3, 4, 8]. One of the operative mechanisms is segregation, very similar to the case of AlG. The enhanced metal solubility in highly phosphorus doped silicon compared to intrinsic silicon has two origins, i.e. (i) the so-called Fermi level effect active for negatively charged metal species – according to current knowledge mainly affecting substitutional metal species M_s –, and (ii) their reaction with phosphorus leading to pairs as e.g. M_sP. These effects have been observed for the 3d transition elements manganese, iron, cobalt [14] and copper [15], as well as for gold [16–18]. Recent experiments for nickel have questioned the existence of an enhanced solubility of nickel in highly P-doped silicon [19]. While both these mechanisms would also be active in the absence of P-diffusion, a third process is intimately linked to non-equilibrium concentrations of intrinsic point defects resulting from fluxes of P-atoms into the silicon [20]. If the diffusion capacity of phosphorus exceeds that of self-diffusion, non-equilibrium concentrations of intrinisic point defects are injected into the

bulk of silicon wafers while their concentrations at the surface remain close to equilibrium values. For P-diffusion it has been shown that self-interstitials are injected due to dissociation of (PI)-pairs in the kink region of typical phosphorus concentration profiles [21–23]. As a result, the gettering effect for metal impurities predominantly dissolved substitutionally is enhanced by a factor corresponding to the ratio $(c_I^{(b)}/c_I^{(0)})$ of self-interstitial concentration in the bulk, $c_I^{(b)}$, to that at the surface, $c_I^{(0)}$. From these considerations it immediately follows that suitable model for phosphorus diffusion itself is a prerequisite for predicitve simulations of metal impurity gettering by PDG. Using these physical models experimental data obtained by Sveinbjörnsson et al. [24] for PDG of gold in silicon could be quantitatively described [25].

The formation of silicide precipitates in the highly P-doped layer has been observed in several studies but has not been described quantitatively up to now [26–29]. It presumably occurs under conditions of phosphorus concentrations exceeding the solubility which leads to the formation of electrically inactive but mobile phosphorus species [30, 31] or even to phosphorus precipitation into SiP [32]. Since such high phosphorus concentrations are usually not applied in solar cell fabrication, this process has not been exploited in photovoltaics up to now. For a more detailed discussion the reader is referred to [3, 4, 8].

2.3 Quantitative modeling and experimental verification

2.3.1 Gettering simulator

The quantitative description of gettering processes and their simulation has two aspects: (i) the redistribution of metal impurities between the silicon bulk and the gettering layers, and (ii) the resulting effect on the electrical properties of the silicon wafer, i.e. finally the performance of the photovoltaic device. These two steps clearly require the development and implementation of suitable *diffusion and gettering models* and a framework describing *excess carrier recombination* at the deep impurities. For AlG, the gettering model is simply the segregation of metal impurities into the Al:Si liquid on the backside of a silicon wafer which simply enters the equations describing transport of metal impurities as a boundary condition. The treatment of PDG requires handling of a complex system involving a suitable model for the phosphorus diffusion itself and the resulting interaction with metal impurities. As described in Section 2.2, the latter can be of electronic origin, a direct reaction of metal species with phosphorus, as well as an indirect interaction via intrinsic point defects produced in non-equilibrium concentrations by the phophorus diffusion process. In subsequent Sections a simulation tool will be used to investigate different processes limiting *gettering kinetics*. It contains the following physical models:

– Phosphorus diffusion is simulated in terms of the model described in detail in Refs. [25] and [5]. Briefly, two mobile phosphorus species are assumed as diffusion vehicles, i.e. (PI)-pairs and a complex containing two phosphorus atoms and a vacancy, i.e. (P_2V). The former is stable in the highly phosphorus doped region but will dissociate in regions of low phosporus concentration leading to self-interstitial injection into the bulk of silicon wafers. The latter prevails in near-surface regions and accounts for the *kink-and-tail form* of typical phosphorus concentration profiles. Due to the coupling of silicon vacancies and interstitials these two species will compete, especially during early stages of phosphorus diffusion.

– Since our present implementation does not aim at describing PDG at phosphorus concentrations exceeding the solubility at gettering temperature, silicide precipitation at the interface between silicon and the phosphorus silica glass has not been included in the gettering model. Hence, the remaining effects to be described are the Fermi-level effect and the formation of pairs between negatively charged substitutional metal species and positively charged phosphorus. The former needs the position of acceptor levels of substitutional metal atoms while the latter is described by the binding energy of the respective pair. For the simulations shown in this work, the assumed parameters are summarized in Table 1. The parameters for PDG of gold have been determined by adjusting the gettering model to experimental data of Sveinbjörnsson et al. [24] while those for cobalt have been chosen in order to fit experimental data of [14, 33, 34]. For PDG simulations involving iron impurities, the properties of cobalt in highly phosphorus doped silicon have been adopted for iron while using the well-known properties of iron in intrinsic

Table 1 Paramaters describing metal impurities at high phosphorus concentration used to simulate PDG in this work. $E^{(\sigma/\sigma-1)}$: position of acceptor level below the conduction band at gettering temperature ($\sigma = 0$, -1, -2); $M^{(\sigma)}(P^{(+)})_n$): dominant metal–phosphorus pair; E_b: binding energy of the dominant pair. The parameters for iron in highly P-doped silicon have been assumed to be identical to those of cobalt (see text).

impurity	$E^{(0/-)}$ [eV]	$E^{(-/2-)}$ [eV]	$E^{(2-/3-)}$ [eV]	$M^{(\sigma)}(P^{(+)})_n$	E_b [eV]
Au	0.55	–	–	$Au_s^{(-)}P^{(+)}$	0.87
Co	0.43	0.37	0.12	$Co_s^{(3-)}(P^{(+)})_2$	1.15

silicon. Hence, the transport kinetics of iron in the bulk of wafers are described properly whereas segregation is taken into account only qualitatively.

– Diffusion of metal impurities in the (intrinsic) bulk of silicon wafers is described in terms of well established models of interstitial diffusion (3d transition elements) or kick-out diffusion (gold or platinum) depending on the impurity under study (for a compilation of diffusion parameters, see [35]).

– One important aspect dealt with in subsequent sections is the dissolution of pre-existing precipitates of metal impurities in solar cell wafers. It is taken into account by adding the reaction of interstitially dissolved metal species with precipitates in a *mean-field approximation,* i.e. a reaction term of type

$$\left(\frac{\partial c_i}{\partial t}\right)_p = \left\langle \frac{c_i^{(eq)}(R_p) - c_i}{\tau(R_p)} \right\rangle, \tag{3}$$

is added to the diffusion equation, where c_i denotes the concentration of interstitial metal atoms and $c_i^{(eq)}$ is the concentration of interstitial metal impurities in equilibrium with a precipitate of radius R_p, $\tau(R_p)$ the reaction time constant, and the brackets on the right hand side indicate averaging over the size-distribution function of the precipitates. The simulations shown in this work have been done assuming a monodisperse size-distribution function and diffusion-limited precipitate growth and dissolution. Hence, possible reaction barriers and precipitate coarsening (Ostwald ripening) are not taken into account. Under such conditions, the reaction time constant is given by

$$\frac{1}{\tau(R_p)} = 4\pi N_p R_p D_i\,, \tag{4}$$

where N_p is the volume density of precipitates and D_i the diffusion coefficient of interstitial metal atoms.

Figure 2 shows an example of a simulated PDG process at 900 °C for gold in silicon, assuming an initial concentration of $c_{Au}(t = 0) = 3 \times 10^{14}$ cm^{-3}. The variation of the gettering time (Fig. 2(a)) shows that under these conditions gettering proceeds from the frontside towards the backside of the wafer.

In order to estimate the effect of gettering on the performance of a solar cell, excess carrier recombination is described in terms of the Shockley–Read–Hall (SRH) model [36, 37]. The resulting depth distribution of carrier lifetime is shown in Fig. 2(b) for the concentration profiles of Fig. 2(a). The successive improvement of carrier lifetime in the front-region of the wafer can be clearly seen. An even more comprehensive form of presenting the effect on the solar cell performance is to calculate the *spectral response (SR)* from the depth profiles of the carrier lifetime [55]. The curves of Fig. 2(c) indicate that the SR especially improves in the long-wavelength (low-energy) regime of incident light which is absorbed in the bulk of the solar cell. Finally, the sheet resistance of the phosphorus doped layer, for the usual design used as the emitter of the solar cell, can be easily calculated from the phosphorus concentration profile. It is thus possible to vary gettering conditions while keeping important solar cell parameters – as the emitter sheet resistance – unchanged. The simulations described in detail in Section 4 are made under such conditions.

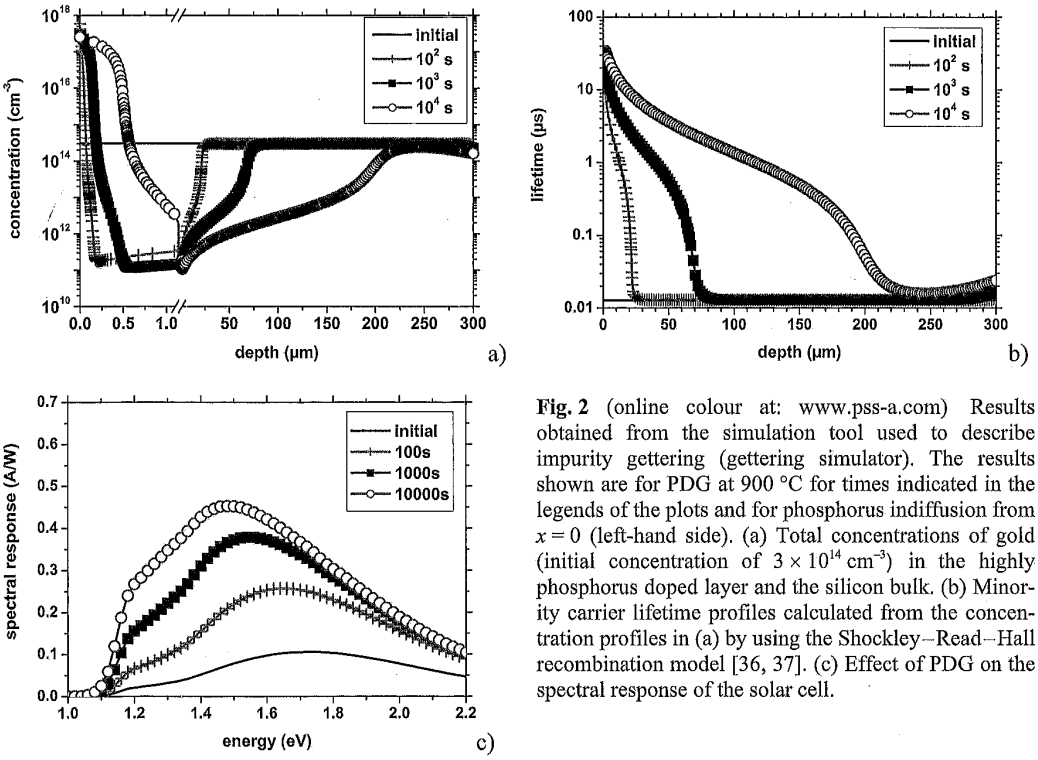

Fig. 2 (online colour at: www.pss-a.com) Results obtained from the simulation tool used to describe impurity gettering (gettering simulator). The results shown are for PDG at 900 °C for times indicated in the legends of the plots and for phosphorus indiffusion from $x = 0$ (left-hand side). (a) Total concentrations of gold (initial concentration of 3×10^{14} cm^{-3}) in the highly phosphorus doped layer and the silicon bulk. (b) Minority carrier lifetime profiles calculated from the concentration profiles in (a) by using the Shockley–Read–Hall recombination model [36, 37]. (c) Effect of PDG on the spectral response of the solar cell.

2.3.2 Quantitative measurements of gettering kinetics

The gettering simulator allows to calculate concentration profiles of individual impurity species, i.e. of the mobile interstitial species (M_i), immobile substitutional species (M_s), precipitated impurities, as well as complexes and pairs with other intrinsic or extrinsic point defects. Experimental techniques measuring concentration profiles of individual species have to be spectroscopic in nature, as e.g. deep level transient spectroscopy. Since reactions between different species will occur during gettering as well as during heating up and cooling down samples to and from gettering temperature, it is difficult to compare the resulting concentration profiles with simulations. In order to measure total concentrations, radioactive techniques like neutron activation analysis or radiotracer activity measurements are at hand. In Section 3 experimental results obtained for cobalt in silicon will be presented. A detailed description of the experimental procedures can be found in [12, 13]. Briefly, radioactive ^{57}Co was diffused into silicon at temperatures between 900 and 960 °C followed by rapid quenching into ethylene glycol. Total cobalt concentrations of $(0.29 - 3.18) \times 10^{13}$ cm^{-3} were measured by counting the 122 keV photons resulting from the $^{57}\text{Co} \rightarrow {}^{57}\text{Fe}$ decay. Near surface precipitates were removed by chemical etching prior to evaporation of Al on one of the surfaces. The gettering anneal was performed in a furnace which had been specially designed for *in-situ* measuring the 6.4 keV X-rays also resulting from the radioactive decay. By aligning the sample with its Al layer towards the detector, the intensity of this radiation is mainly given by the amount of cobalt gettered into the Al:Si melt since the penetration depth of 6.4 keV X-rays for silicon is only 24.6 μm. Hence, the gettering effect is measured during annealing at high temperature avoiding the interference of the results with impurity redistribution during cooling which may be difficult to control.

3 Gettering efficiency and kinetics – limiting factors

In this section, physical processes limiting the efficiency and kinetics of impurity gettering will be discussed. They will be analysed by means of simulations and experimental results obtained for cobalt in silicon. Special emphasis will be on the role of immobile metal species, in particular metal silicide precipitates.

3.1 Formation of gettering layer

Since the main effect of AlG and PDG under conditions usually applied in silicon solar cell fabrication is due to segregation, the time necessary to form the respective gettering layer will affect gettering kinetics. For AlG, the Al:Si melt with composition corresponding to the equilibrium with silicon at gettering temperature has to be formed. From gettering kinetics measured for fast diffusing cobalt in silicon (see also Section 3.3) it could be concluded that the gettering layer forms instantaneously from the evaporated Al films reacting with silicon. Since diffusion in liquids usually is very fast, one may conclude that the gettering layer in this case already forms during heating up the silicon wafer to gettering temperature.

The situation is different for PDG since phosphorus diffusion – and hence the formation of the gettering layer – is a slow process especially when compared to diffusion of the highly mobile interstitial impurities cobalt, nickel or copper. Figure 3 summarizes simulations of PDG for model impurities which have identical properties in the highly phosphorus doped layer, i.e. those given for cobalt in Table 1, but diffusion coefficients in intrinsic silicon corresponding to those of iron, cobalt, and copper at 900 °C. It is assumed that all impurity atoms are dissolved interstitially (initial concentration: 10^{14} cm^{-3}, wafer thickness: 300 μm) at gettering temperature. For short gettering times, the amount of gettered metal impurities is limited by their diffusivity while for long times a quasi-stationary state is reached which can be described by a $t^{-1/2}$-power law for the fraction of metal impurities remaining in the wafer. In this regime, gettering kinetics are limited by the indiffusion of phosphorus which is corroborated by the temporal evolution of the emitter sheet resistance shown in Fig. 3 (right scale). It should be noted that this quasi-stationary state is reached within about 100 s for the fast diffusors but takes approximately 1 h for the model impurity with diffusion properties of interstitial iron in intrinsic silicon.

3.2 Diffusivity of mobile species

For completion, this section considers the diffusivity of interstitial metal atoms as a limiting factor of gettering kinetics. A more thorough treatment of this aspect can be found in [5]. For a given impurity, gettering kinetics are ultimately limited by the diffusion coefficient of the interstitial species if one assumes that all metal atoms are mobile and gettering layers form instantaneously. A rough estimate of this

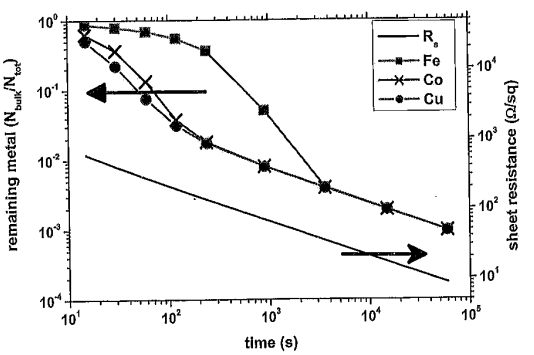

Fig. 3 (online colour at: www.pss-a.com) Simulation of phosphorus diffusion gettering kinetics: the fraction of metal impurities left in the bulk is shown for metal impurities with interstitial diffusion coefficients corresponding to those of iron (solid squares), cobalt (crosses), and copper (solid circles). For short times, gettering kinetics are limited by the diffusion of metal impurities, whereas phosphorus indiffusion is the limiting process for long times. The latter are characterised by a time law $\propto t^{-1/2}$ which also describes the time-dependence of the sheet resistance R_s (solid line, right scale). Please note the logarithmic scale of the gettering time.

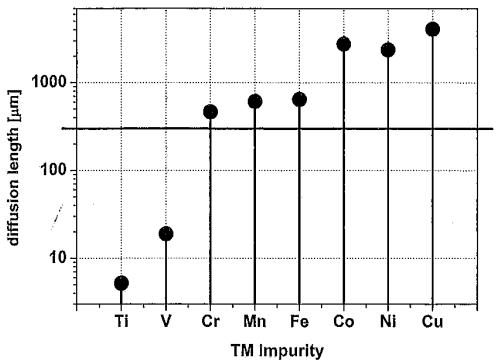

Fig. 4 For efficient external gettering of metal impurities by means of phosphorus diffusion or aluminum, the diffusion length of interstitial metal species has to be on the order of the wafer thickness. The plot summarizes data for 30 min at 850 °C for various 3d transition elements in silicon [35]. The horizontal line at 300 µm indicates that the 3d elements from Cr to Cu can be gettered whereas the mobility of Ti and Sc is much too small for gettering to be efficient.

effect is to compare the diffusion length L_{Mi} of interstitial metal atoms with the thickness d of the solar cell wafer: if external gettering is to be effective, L_{Mi} has to be on the order of d. Figure 4 compares these quantities for the 3d transition elements from Ti to Cu. For the fast diffusors cobalt, nickel and copper, $L_{Mi} \gg d$ is fulfilled and $L_{Mi} > d$ still holds for chromium, manganese and iron. The much smaller mobility of the light 3d elements prevents external gettering procedures to be effective for these impurities.

3.3 Immobile species

Transport of metal impurities during gettering is always carried by the mobile interstitial metal species M_i. In addition, metal impurities may be present in several forms of immobile species which do not contribute to diffusion. Instead, the effective diffusion coefficient D_{eff} may be much smaller than the interstitial diffusion coefficient D_i as can be estimated from the relation

$$D_{eff} = \frac{c_i D_i}{c_i + c_{im}}, \tag{5}$$

where c_{im} is the total concentration of all immobile species. In addition, immobile species may act as a persistent source of interstitial metal atoms which is especially important if M_i is the dominant electrically active species accounting for the impurity effect on minority carrier lifetime as for the 3d elements from titanium to iron. In subsequent sections, we shall consider substitutional metal species, precipitated impurities, complexes of metal atoms and other impurities, and finally the interaction with extended defects, in particlar dislocations.

3.3.1 Substitutional species

The 3d transition metal impurities are predominantly dissolved on interstitial sites in intrinsic silicon implying that their transport is independent of the presence of intrinsic point defects serving as diffusion vehicles. This is considerably different for impurities like zinc, platinum and, as the most prominent example, gold. These elements predominantly dissolve on substitutional sites also in intrinsic silicon. In order to illustrate the effect of substitutional species on gettering kinetics, we briefly discuss PDG of gold in silicon. A more detailed investigation has been reported in [25]. In the framework of the kick-out mechanism which is operative for gold diffusion the mobile species Au_i is produced by the reaction

$$Au_s + I \rightleftharpoons Au_i, \tag{6}$$

where I denotes silicon self-interstitials. Hence, a supersaturation of self-interstitials will enhance the gettering kinetics for gold. Figure 5 shows concentration profiles of substitional gold and silicon self-interstitials for PDG at 900 °C for 2 h. The main feature of the Au_s concentration profile is a steep step at a depth corresponding to the penetration depth of I which, in turn, is mainly determined by the gold con-

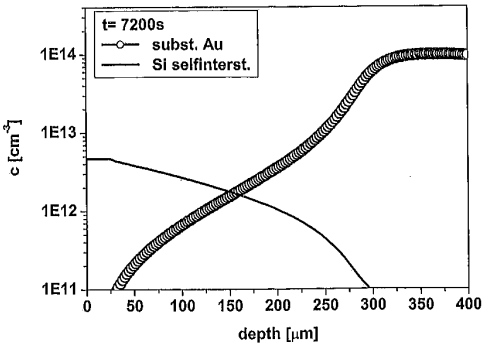

Fig. 5 (online colour at: www.pss-a.com) Simulation of PDG of gold in silicon at 900 °C for 2 h. The concentration profiles of substitutional gold (open circles) and of silicon self-interstitials (solid line) in the bulk of the wafer show the effect of self-interstitial injection from phosphorus indiffusion. Due to the high initial gold concentration of 10^{14} cm^{-3} the self-interstitial diffusion is *trap-limited* by the reverse *kick-out* reaction.

centration itself since the effective diffusion coefficient of I is limited by the reaction Eq. (6). Finally, it should be noted that the self-interstitial supersaturation produced by the phosphorus diffusion process has beneficial effects on gettering kinetics as well as on the gettering efficiency (compare Section 2.2).

3.3.2 Metal silicide precipitates

Multicrystalline silicon materials for photovoltaic applications contain extended defects like grain boundaries, dislocations and microdefects. Such defects are known to serve as nucleation sites for transition metal impurity precipitates mainly in form of metal silicides (see [9] for a recent review). Since crystal growth inevitably involves slow cooling from high temperature, metal impurities are expected to be mainly present in form of precipitates in solar cell wafers. In a series of recent experiments this expectation has been proven by means of synchroton-based spatially resolved chemical analysis [38].

In order to remove precipitated metal impurities by external gettering, precipitates have to be dissolved and interstitial metal species emitted by precipitates have to diffuse to the gettering layer and accumulate there. The dissolution reaction (Eq. (3)) will slow down gettering kinetics and ultimately limit the process. Close inspection of Eqs. (3) and (4) reveals that the reaction term is governed by two properties, i.e.

– the relative magnitude of the concentration c_i of M_i and the concentration $c_i^{(eq)}(R_p)$ in equilibrium with a precipitate of radius R_p, and

– the density N_p and size R_p of precipitates.

For experimental investigations of the dependence of gettering kinetics, conditions have to be chosen such that all other rate-limiting processes can be excluded. For this reason AlG has been chosen instead of PDG since the time to form the gettering layer is small compared to the total gettering time. In fact, the Al:Si liquid seems to form already during heating the sample to gettering temperature, T_G. Furthermore, immobile metal species in addition to precipitates have to be excluded so that dislocation-free float-zone silicon materials have been used. Since total metal concentrations have to be measured the radiotracer technique described in Section 2.3.2 has been applied for cobalt impurities. It is well known that cobalt predominantly precipitates during or after cooling from high temperature unless high concentrations of shallow acceptors are present [33, 39]. Hence, at room temperature practically all cobalt atoms have precipitated which is the starting point of any gettering experiment. During heating up the sample to T_G and during subsequent annealing, precipitates will dissolve to the extent that the equilibrium concentration $c_i^{(eq)}(R_p)$, approximated by the solubility $c_i^{(eq)}$ in the following, is established in the sample. These considerations show that two limiting cases can be distinguished, i.e. $c_{tot} < c_i^{(eq)}(T_G)$ or $c_{tot} > c_i^{(eq)}(T_G)$, where c_{tot} is the total cobalt concentration. In the former case all precipitates have to dissolve in order to establish the solubility at gettering temperature, in the latter precipitates will still be present even if the solubility is established. Figure 6 compares AlG kinetics of cobalt for $c_{tot} < c_i^{(eq)}(T_G)$ (filled squares) and $c_{tot} > c_i^{(eq)}(T_G)$ (open circles) and with a simulation calculated assuming that all cobalt impurities are interstitially dissolved (solid line) which is equivalent to assuming that AlG is limited by interstitial cobalt

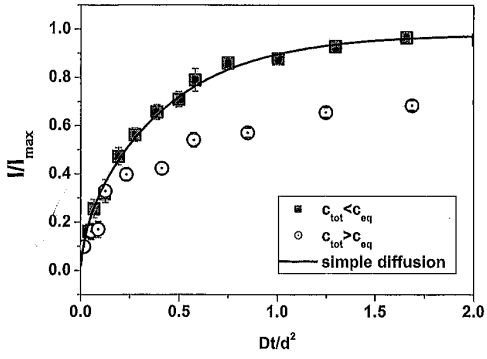

Fig. 6 (online colour at: www.pss-a.com) AlG kinetics of cobalt in float zone silicon for different ratios of total cobalt concentration c_{tot} and solubility c_{eq} at gettering temperature. $c_{tot}/c_{eq} < 1$: experimental data (squares) and model of simple outdiffusion (line) showing that precipitate dissolution does not limit gettering kinetics. $c_{tot}/c_{eq} > 1$: experimental data (open circles) showing that precipitate dissolution considerably slows down gettering kinetics. Please note that the reduced gettering time Dt/d^2 has been used, where D is the diffusion coefficient at gettering temperature and d is the sample thickness.

diffusion [40]. It is clearly seen that gettering kinetics are as fast as simple outdiffusion of completely dissolved interstitial cobalt for $c_{tot} < c_i^{(eq)}(T_G)$ which provides evidence that in this case precipitate dissolution has to be completed at a very early stage of gettering, or even during heating up to gettering temperature. On the contrary, for $c_{tot} > c_i^{(eq)}(T_G)$ gettering kinetics significantly lag behind pure outdiffusion, i.e. precipitate dissolution is the rate-limiting process.

The effect of precipitate density and size on gettering kinetics has been verified by a second set of experiments described below. For a given total cobalt concentration, the product $N_p R_p^3$ of cobalt silicide precipitates at room temperature has to be constant. As a consequence, the time-constant $\tau(R_p)$ for precipitate dissolution will be proportional to $N_p^{-2/3}$ implying that gettering kinetics should slow down with decreasing precipitate density (or increasing precipitate size). Figure 7 shows AlG kinetics for cobalt at $T_G = 806$ °C for a total concentration of $c_{tot} = 6 \times 10^{12}$ cm^{-3} equal to the solubility of cobalt at that gettering temperature $c_i^{(eq)} = 6 \times 10^{12}$ cm^{-3} according to [41]. The two samples differ by their thermal treatment prior to AlG, namely by pre-annealing at 670 °C which is known to lead to precipitate coarsening (Ostwald ripening) [33, 42]. It is evident that gettering is considerably slower for the sample with pre-anneal (open circles) compared to that without (solid squares).

3.3.3 Complex formation

Non-metallic impurities like carbon, oxygen, and nitrogen are present in different silicon materials in different concentrations. Interaction of metal impurities with point or extended defects associated with these impurities is a wide field. In particular, extended defects resulting from oxygen precipitation in Czochralski grown silicon promote precipitation of metal impurities, the underlying process of internal gettering used in silicon microelectronics. First evidence for the formation of complexes between cobalt

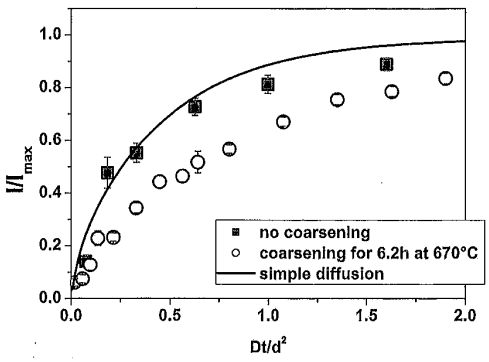

Fig. 7 (online colour at: www.pss-a.com) AlG kinetics at 806 °C of cobalt in float zone silicon for different initial precipitate densities. The initial cobalt concentration of $c_{ini} = 6.0 \times 10^{12}$ cm^{-3} is equal to the solubility at gettering temperature, $c_{eq}(T = 806\ °C) = 6.0 \times 10^{12}$ cm^{-3}. The two samples differ by the precipitate coarsening treatment at $T = 670$ °C prior to AlG: no coarsening (solid squares) and coarsening for 6.2 h (open circles). The solid line describes simple outdiffusion, for comparison. It is clearly seen, that a reduction of the precipitate density by the coarsening treatment slows down the gettering kinetics.

and oxygen-related centers (OX-centers) *at high temperature* has been reported recently [13]. In these experiments, radioactive ^{57}Co was diffused into oxygen-rich Cz-Si ($[O_i] = 7.8 \times 10^{17}$ cm^{-3}, new AST) which was annealed for 1 h at 1310 °C prior to cobalt doping in order to dissolve pre-existing oxygen precipitates and complexes. After quenching to room temperature, chemical removal of surface layers, samples were subjected to a gettering treatment using a liquid Au:Si layer instead of the Al:Si melt used in AlG [43]. Using the temperature cycling procedure described in Section 2.3.2, cobalt impurities were redistributed between the silicon and the gettering layer. Unlike for FZ-Si where decreasing temperature always results in an increasing amount of gettered cobalt, back-diffusion of cobalt atoms from the gettering layer to the silicon was observed for oxygen-rich silicon when the gettering temperature was lowered below $T_{OX} = 930$ °C. This *inverse gettering* is associated with a strongly decreasing effective diffusion coefficient of cobalt in silicon. Both phenomena provide evidence that immobile complexes of cobalt and OX-centers form below T_{OX}. Inverse gettering was also observed for oxygen-rich multicrystalline silicon with similar oxygen content usually found near the bottom of block-cast materials.

3.4 Interaction with extended defects

Extended defects like grain boundaries and dislocations play an important role for the electrical performance of multicrystalline silicon materials. Both serve as heterogeneous precipitation sites which is the reason that those regions contain high concentrations of metal precipitates or clusters [44]. It is well accepted to date that the recombination activity of dislocations is closely related to deep level defects in or in the direct vicinity of the dislocation core [10]. They can be due to intrinsic core defects or due to metal impurity atoms as presumably the dominant source. The latter can segregate in the strain field of dislocations or form 'chemical' bonds with the dislocation core [9, 45]. Recent studies of dislocation luminescence in silicon have demonstrated an impressive enhancement of the so-called *D1 luminescence* [46] at room temperature as a result of suitable gettering and passivation processes [47, 48]. This enhancement of dislocation luminescence is associated with a strong reduction of deep levels serving as non-radiative recombination centers competing with the D1-luminescence.

If gettering kinetics of metal impurities at dislocations are to be described quantitatively and to be included in predictive simulations the predominant type of interaction has to be identified, binding energies of impurities to dislocations have to be determined and the electronic structure of metal atoms close to or in dislocation cores has to be studied. For conclusive experiments in this field, at least two problems have to be solved, i.e.

– to distinguish the effects of metal impurities on the deep level spectrum of dislocations from those produced by thermal treatments and undeliberate contamination, and

– to distinguish between deep level centers in the undisturbed bulk from those located close to dislocations.

The latter problem has to be solved by spectroscopic techniques. In fact, deep level transient spectroscopy, DLTS, has been shown to be sensitive to the environment of point defects [49]. On the one hand, capture kinetics provide a fingerprint of whether point defects are isolated or linked via a common charge-dependent Coulomb potential. On the other hand, emission characteristics allow to distinguish localised and bandlike extended defects as well as – for localized extended defects – provide some insight into the relative response to the dislocation strain field of the deep level point defect and of the band to which charge carriers are emitted in the DLTS experiment, i.e. the conduction and valence band for n- and p-type semiconductors, respectively [45]. The former problem has been tackled recently by deliberately introducing metal impurities into dislocated silicon by diffusion and subsequent DLTS measurement at different depths in the sample corresponding to different metal impurity concentrations [50]. Using this approach it could be shown that gold most probably segregates in the strain field of dislocations. Figures 8(a) and (b) show DLTS spectra from dislocated n-type silicon corresponding to low and high gold concentration, respectively. In addition to the well-known dislocation-related C-lines, a signal (labelled "Au" in Fig. 8(b)) was detected in regions of high gold concentration which was absent in regions of small gold concentration [50]. The emission characteristics of the line correspond to those of the gold

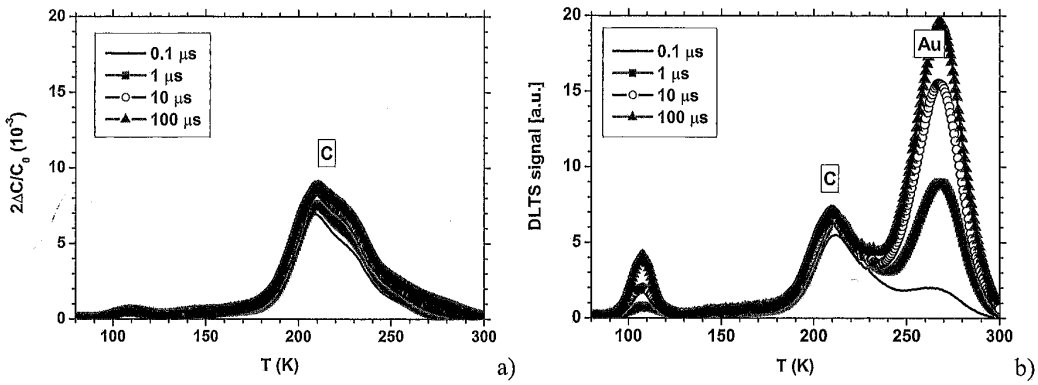

Fig. 8 (online colour at: www.pss-a.com) DLTS of gold in dislocated n-type silicon. (a) Low gold concentration showing mainly dislocation-related C-lines. (b) High gold concentration showing a near-midgap level as the dominant defect besides the dislocation-related C-lines. Electron emission from the near-midgap level shows properties practically identical to those of the gold acceptor level in dislocation-free silicon. The logarithmic capture kinetics provide evidence that gold has accumulated close to dislocations.

acceptor in dislocation-free silicon whereas logarithmic capture kinetics provide evidence for the extended nature of the defects. It has been concluded that such behaviour is in agreement with gold atoms in the strain field of dislocations rather than in the dislocation core. Recent experiments on gold diffused dislocated p-type silicon have shown similar results for the gold donor level and, in addition, revealed a more shallow level with logarithmic capture kinetics and a concentration very close to that of the gold donor level [51].

Such experiments are readily extended to 3d transition element impurities with the additional complication, however, that their tendency to form silicide precipitates at dislocations and thus vanish from solution. Nevertheless, a framework for experiments has been developed which possibly allows to study not only the electronic structure of metal impurities at dislocations but also to study redistribution kinetics of impurities between the undisturbed bulk and the dislocations. Hence, the estimation of binding energies of metal impurities to dislocations – a prerequisite for quantitatively including such defects into gettering simulations – seems to be feasible.

4 Alternative proccessing schemes

Standard processing schemes for silicon solar cells produced on p-type materials include furnace annealing steps for emitter diffusion and back-surface field formation which simultaneously serve as PDG and AlG steps, respectively. There is recent interest in alternative processing involving in particular *rapid thermal processing, RTP*. Annealing times of phosphorus diffusion could be reduced to several seconds at e.g. 1100 °C with the emitter sheet resistance still in the range of typical furnace anneling conditions. From the physical considerations outlined in Section 2 it is evident that the efficiency of PDG will be significantly reduced due to the decreasing segregation effect with increasing temperature. In addition, the diffusion length of metal impurities will be smaller compared to typical furnace annealing processes since their diffusion coefficient is much less thermally activated as the effective diffusivity of phosphorus in silicon. Figure 9 shows the results of a PDG simulation for a model impurity with properties of interstitial iron in intrinsic silicon and those of cobalt in highly phosphorus doped silicon (compare Table 1). The concentration profiles (Fig. 9(a)) for the silicon bulk demonstrate the reduced gettering efficiency of the RTP process at 1100 °C compared to the furnace annealing at 900 °C. Comparison of the resulting SR curves emphasize that RTP gettering hardly improves the electrical performance of the material. Please note, that conditions were chosen such that the emitter sheet resistance was identical in the two cases.

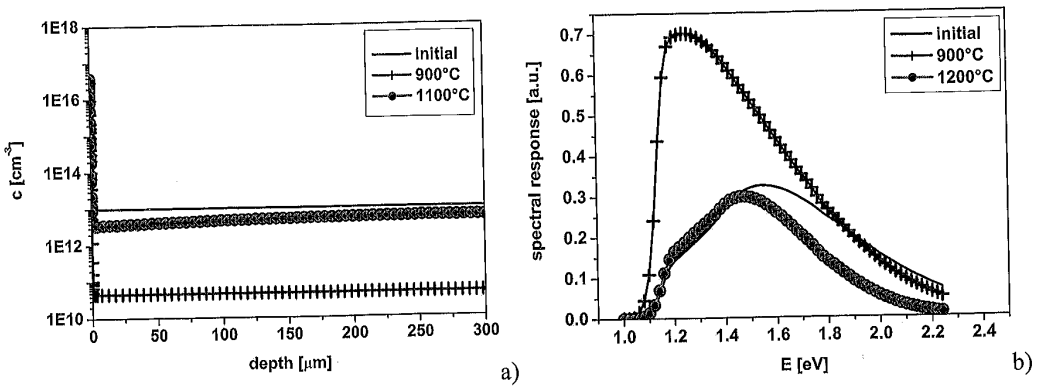

Fig. 9 (online colour at: www.pss-a.com) Reduced gettering efficiency due to high-temperature RTP. (a) Metal impurity concentration profiles in the bulk of a silicon wafer subjected to PDG at 900 °C and 1100 °C for times establishing a fixed sheet resistance of 20 Ω/sq. (b) Resulting changes of the 'Spectral Response' showing almost no effect of RTP gettering.

In a recent paper, Buonassisi and coworkers [52] have shown that RTP of multicrystalline silicon electrically degrades the material. They could further show that degradation is due to the dissolution of metal silicide precipitates – especially iron silicide – located at grain boundaries.

In this section, the reduced gettering effect during RTP will be demonstrated for conditions where all metal impurities are interstitially dissolved (Sec. 4.1). It will be further shown that a two-step annealing scheme allows to recover the gettering efficiency typical for furnace annealing. In Section 4.2 gettering simulations will be extended to the case that metal impurities are condensated into silicide precipitates. We show there that a RTP two-step process can possibly be beneficial for silicon materials containing metal silicide precipitates.

4.1 Rapid thermal gettering – interstitially dissolved impurities

In order to restore gettering efficiency in processing schemes involving RTP, possible variants are the combination with a low-temperature gettering annealing, i.e. a two-step process, or the use of slow temperature ramping from RTP temperature. In the remaining of this section, simulations are presented which demonstrate this statement taking the example of a two-step process. The simulations are carried out for the model impurity with properties of interstitial iron in intrinsic silicon and those of interstitial cobalt in highly phosphorus doped silicon. Gettering conditions have been chosen as a RTP-step at $T_D = 1100$ °C followed by a second annealing at $T_G = 800$ °C. The maximum annealing time t_{max} at T_D necessary to establish an emitter sheet resistance of about 20 Ω/sq without subsequent 800 °C annealing is used to introduce the normalized annealing time $t_n = t/t_{max}$. Annealing times at T_D and T_G have been chosen such that the thermal budget for phosphorus diffusion remains unchanged, i.e. the emitter sheet resistance was fixed. The concentration profiles summarized in Fig. 10(a) reveal the reduced gettering effect for RTP gettering ($t_n = 1$) and the significant reduction of the contamination level if the second annealing step at $T_G = 800$ °C is added to the process. Subsequently, this second step will be referred to as the *gettering step*. The maximum gettering effect to be achieved is realised by a single-step process at T_G without prior RTP. Practically the same effect is reached for $t_n = 0.4$ implying that a reduction of the *total* processing time can be achieved by the two-step process leaving the gettering effect and the emitter properties unchanged. An enhanced gettering effect, however, is not expected from such two-step processing if only interstitially dissolved metal impurities are taken into account.

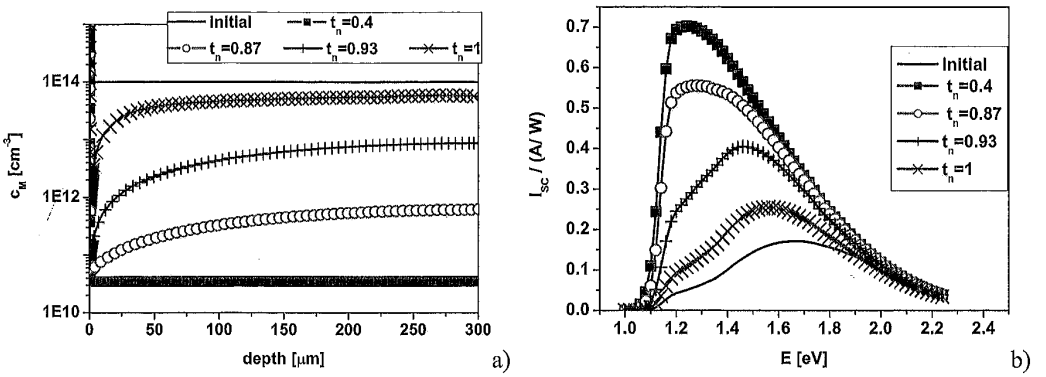

Fig. 10 (online colour at: www.pss-a.com) Simulation of a two-step gettering process consisting of RTP at T_D = 1100 °C followed by a gettering anneal at T_G = 800 °C resulting in a fixed emitter sheet resistance. It is assumed that all metal impurities are dissolved on interstitial sites at the respective annealing temperature. RTP annealing time has been normalized to the case without subsequent 800 °C annealing step. (a) Concentration profiles of metal impurities. (b) Resulting spectral response. The improved gettering efficiency of the increasing 800 °C-annealing fraction of the total thermal budget is clearly seen. It should be noted, that for *completely dissolved* metal impurities, RTP has no beneficial effect compared to furnace annealing.

4.2 Rapid thermal gettering – precipitated impurities

The situation changes if metal impurity precipitates are taken into account which will be shown below. Bearing in mind the results of Buonassisi and coworkers [52] that impurity atoms released from silicide precipitates during RTP may electrically degrade solar cell materials, two strategies are at hand, i.e. to anneal at such low temperature during solar cell manufacturing that precipitate dissolution is kept at a minimum [52] or to dissolve the precipitates and redistribute the mobilized impurities by a suitable gettering scheme. The experimental results described in Section 3.3.2 have quantitatively shown that the relative magnitude of the total metal concentration, c_{tot}, and the equilibrium concentration $c_i^{(eq)}$ at gettering temperature mainly determine gettering kinetics. For fast precipitate dissolution, the annealing temperature has to exceed T_{diss} defined by the condition $c_{tot} = c_i^{(eq)}(T_{diss})$.

The dependence of T_{diss} on impurity concentration is shown in Fig. 11 for different metals. For illustration let us assume a total metal concentration $c_{tot} = 10^{14}$ cm^{-3} indicated by the vertical line. It is apparent

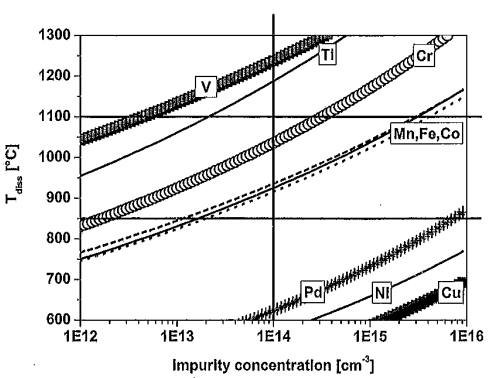

Fig. 11 (online colour at: www.pss-a.com) Temperature necessary to dissolve metal silicide precipitates in silicon as a function of the total metal impurity concentration. Two horizontal lines indicate processing temperatures of typical furnace annealing (850 °C) and of typical RTP (1100 °C). Roughly three groups of impurities can be identified if a typical metal concentration of $c_{tot} = 10^{14}$ cm^{-3} is assumed. Silicide precipitates of nickel, copper, and palladium dissolve during furnace annealing, whereas those of cobalt, iron, manganese and also chromium are stable under these conditions but dissolve at 1100 °C. Precipitates of the third group (Ti, V) should be stable at even higher temperature.

that silicide precipitates of nickel, copper, and palladium will dissolve even at a typical furnace annealing temperature of 850 °C (solid horizontal line) where segregation is effective for both PDG and AlG implying that such precipitates can be effectively removed, in agreement with experimental results [52]. For cobalt, iron, manganese and in particular chromium, higher temperatures are needed, i.e. temperature where segregation in general and hence the efficiency of PDG and AlG is reduced.

In order to dissolve precipitates *and* remove the dissolved impurities by gettering, a two-step processing scheme involving high-temperature RTP annealing (dissolution step at T_D) followed by low-temperature annealing (gettering step at T_G) under the constraints of a fixed emitter sheet resistance is feasible as will be shown below by means of a gettering simulation study. It has been done under the condition of an emitter sheet resistance $R_s = 20\ \Omega$/sq, a RTP step at $T_D = 1100$ °C followed by a gettering step at $T_G = 800$ °C. Hence, for a given RTP annealing time, the duration of the subsequent gettering step is given by the condition of fixed R_s. The results will be presented by plotting total metal concentration c_{tot} and precipitate density N_p vs. RTP annealing time t/t_{max} normalized to t_{max} which is the RTP processing time necessary to establish the sheet resistance without subsequent gettering step. In Section 3.3.2 it has been discussed in some detail that precipitate dissolution kinetics will depend on density and size of precipitates which are linked if – as assumed here – all metal impurities have precipitated prior to the two-step annealing:

$$c_{tot}\ (t=0) = c_{max} = \frac{4\pi}{3\Omega} R_p^3 N_p\,, \tag{7}$$

where Ω denotes the volume per metal atom in the spherical metal silicide precipitate of radius R_p and density N_p. The simulations have been performed for a fixed impurity concentration in precipitates with a low, medium and high density. In Fig. 12(a) the total metal concentration (normalized to the initial value) is plotted vs. the normalized annealing time at dissolution temperature T_D. Qualitatively, the metal concentration decreases with increasing RTP annealing time, reaches a plateau on a low concentration level and increases again for large t/t_{max}. The interpretation of this behaviour is straight forward, if the time-dependence precipitate density is taken into account (Fig. 12(b)). For short times, precipitate dissolution at T_D is incomplete leading to incomplete gettering of impurities at T_G where the equilibrium

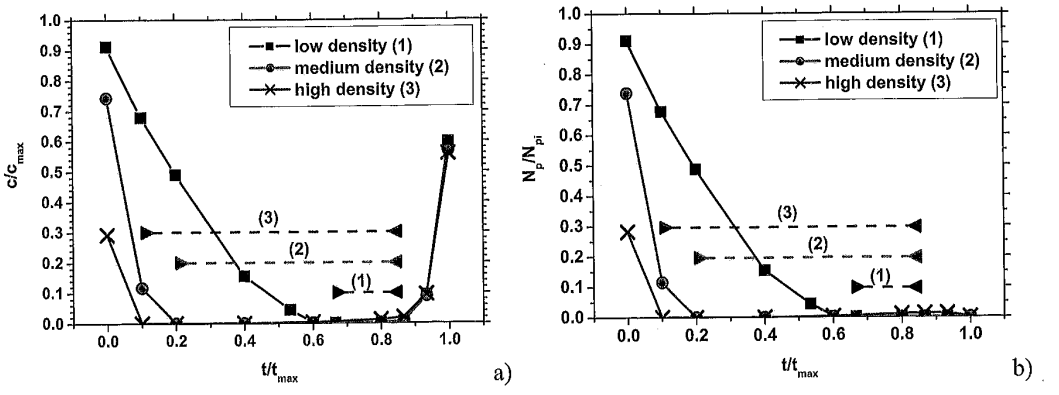

Fig. 12 Simulation of a two-step gettering process consisting of RTP at $T_{diss} = 1100$ °C followed by a gettering anneal at $T_G = 850$ °C. The duration t of the RTP step and the subsequent gettering step have been chosen such that the sheet resistance of the P-doped emitter remained constant. (a) Total concentration c of metal impurities as a function of RTP-time t, and (b) precipitate density N_p as a function of RTP-time t for three different initial precipitate densities N_{pi} for a fixed initial impurity concentration c_{tot} $(t=0) = c_{max}$. The time t_{max} corresponds to the P-diffusion time at $T = 1100$ °C necessary to establish the sheet resistance without subsequent gettering step. Dashed arrows indicate processing windows for complete metal impurity gettering for different initial densities of precipitates. Please note that $t = 0$ refers to gettering anneal only without prior RTP treatment.

concentration is below the total metal concentration leading to slow gettering kinetics (compare Section 3.3.2 for experimental results). For long times, dissolution of precipitates is complete, the remaining gettering at T_G, however, is too short to remove impurities from the bulk of the wafers. It should be noted that points at $t = t_{max}$ correspond to RTP gettering only. It is obvious that the plateau regions forming for intermediate RTP times correspond to a processing window which allows almost complete removal of metal impurities. Finally, it should be mentioned that instead of a two-step processing scheme, temperature ramping from T_D to room temperature can be adjusted such that the same gettering effect can be achieved.

5 Summary and conclusion

In summary, this paper has described the current state of understanding, modeling and experimental verification of gettering techniques mainly used in silicon photovoltaics, namely phosphorus diffusion gettering, PDG, and aluminum gettering, AlG. Special emphasis has been put on factors limiting gettering efficiency and kinetics. For the ubiquitously present 3d transition metal impurities these are silicide precipitates, binding to extended defects like dislocations, and formation of complexes with non-metallic impurities.

As precipitation is concerned, the relative magnitude of the total metal impurity concentration and the solubility at gettering temperature as well as the size and density of the precipitates determine gettering kinetics as has been verified experimentally for AlG of cobalt. First evidence for a binding between cobalt and oxygen-related centers has been presented which leads to the important phenomenon of 'inverse gettering' which is the backdiffusion of cobalt atoms into the silicon in order to establish a new stationary state in the presence of OX-centers. Further experiments are needed to identify the type of OX-centers involved in complex formation and also to check whether binding to OX-centers is a general phenomenon operative for other 3d transition metal atoms, too.

Binding to dislocations is another important issue for solar cell silicon materials. An experimental framework has been set up which makes investigations of binding energies, segregation kinetics as well as of the effect of metal impurities on the deep level spectrum of dislocations feasible. For the case of gold it has been shown that segregation in the dislocation strain field seems to be the dominant type of interaction. Although it has been demonstrated that a suitable combination of gettering and passivation is able to reduce non-radiative carrier recombination at dislocations to such an extent that radiative recombination becomes efficient even near room temperature [47, 48], this field has still not reached the level of quantitative understanding and modeling.

Finally, alternative processing schemes involving RTP have been explored for their potential to effectively remove precipitated metal impurities. A two-step processing scheme consisting of a dissolution step realized by RTP followed by a gettering step at lower temperature has been described and a processing window has been shown to exist even if processing constraints of a fixed thermal budget for phosphorus diffusion are applied. Instead of the two-step scheme, an alternative combination of precipitate dissolution by RTP followed by controlled cooling to room temperature leads to identical results. Experimental verification of these processing schemes are a future task although strong evidence for the beneficial effect of slow cooling after high-temperature annealing has been presented previously [53, 54]: in a series of experiments it was shown that as-grown block cast silicon materials electrically degrade if (furnace) annealed at 1200 °C and subsequently *quenched* to room temperature. The same annealing conditions followed by slow cooling, however, recovered the initial diffusion length. These results were interpreted in terms of metal impurity release from precipitates during 1200 °C annealing and their re-precipitation during slow cooling and staying in solution or forming high densities of small clusters during quenching. Therefore, it might be concluded that the detrimental effect of high-temperature RTP is closely related to fast cooling typical for RTP rather than the high temperature treatment alone. Clearly, more experiments are necessary to clarify this point and to explore whether a robust processing scheme involving RTP and effective gettering can be established.

Acknowledgements This work was financially supported by the Volkswagen Foundation (SOBSI project) and the German Ministry for Environement, BMU, under contract no. 329858B.

References

[1] A. A. Istratov, T. Buonassisi, R. J. McDonald, A. R. Smith, R. Schindler, J. A. Rand, J. P. Kalejs, and E. R. Weber, J. Appl. Phys. **94**, 6552 (2003).
[2] T. Y. Tan, E. E. Gardner, and W. K. Tice, Appl. Phys. Lett. **30**, 175 (1977).
[3] S. M. Myers, M. Seibt, and W. Schröter, J. Appl. Phys. **88**, 3795 (2000).
[4] W. Schröter, M. Seibt, and D. Gilles, in: Handbook of Semiconductors Vol. 1, edited by W. Schröter and K. Jackson (Wiley-VCH, Weinheim, 2000), p. 597.
[5] W. Schröter, V. Kveder, M. Seibt, A. Sattler, and E. Spiecker, Sol. Energy Mater. Sol. Cells **2002**, 299 (2002).
[6] P. S. Plekhanov, R. Gafiteanu, U. M.Gösele, and T. Y. Tan, J. Appl. Phys. **86**, 2453 (1999).
[7] P. S. Plekhanov, M. D. Ngoita, and T. Y. Tan, J. Appl. Phys. **90**, 5388 (2001).
[8] W. Schröter, A. Döller, A. Zozime, V. Kveder, M. Seibt, and E. Spiecker, Solid State Phenom. **95/96**, 527 (2004).
[9] M. Seibt, V. Kveder, W. Schröter, and O. Voss, phys. stat. sol. (a) **202**, 911 (2005).
[10] V. Kveder, M. Kittler, and W. Schröter, Phys. Rev. B **63**, 115206 (2001).
[11] M. Apel, I. Hanke, R. Schindler, and W. Schröter, J. Appl. Phys. **76**, 4433 (1994).
[12] A. Sattler, PhD Thesis, Göttingen 2003 (Cuvillier, Göttingen 2002, ISBN 3-89873-856-6).
[13] A. Sattler, M. Seibt, V. Kveder, and W. Schröter, Solid State Phenom. **95/96**, 553 (2004).
[14] D. Gilles, W. Schröter, and W. Bergholz, Phys. Rev. B **41**, 5770 (1990).
[15] R. N. Hall and H. Racette, J. Appl. Phys. **35**, 379 (1964).
[16] L. Baldi, G. F. Cerofolini, G. Ferlsy, and G. Frigerio, phys. stat. sol. (a) **48**, 523 (1978).
[17] S. F. Cagnina, J. Electrochem. Soc. **116**, 498 (1969).
[18] T. A. O'Shaughnessy, H. D. Barber, D. A. Thompson, and E. L. Heasell, J. Electrochem. Soc. **121**, 1350 (1974).
[19] A. A. Istratov, P. Zhang, R. J. McDonald, A. R. Smith, M. Seacrist, J. Moreland, J. Shen, R. Wahlich, and E. R. Weber, J. Appl. Phys. **97**, 023505 (2005).
[20] E. Spiecker, M. Seibt, and W. Schröter, Phys. Rev. B **55**, 9577 (1997).
[21] F. F. Morehead and R. F. Lever, Appl. Phys. Lett. **48**, 151 (1986).
[22] B. J. Mulvaney and W. B. Richardson, Appl. Phys. Lett. **51**, 1439 (1987).
[23] M. Orlowski, Appl. Phys. Lett. **53**, 1323 (1988).
[24] E.Ö. Sveinbjörnsson, O. Engström, and U. Södervall, J. Appl. Phys. **73**, 7311 (1993).
[25] V. Kveder, W. Schröter, A. Sattler, and M. Seibt, Mater. Sci. Eng. B **71**, 175 (2000).
[26] A. Ourmazd and W. Schröter, Appl. Phys. Lett. **45**, 781 (1984).
[27] A. Ourmazd and W. Schröter, Mater. Res. Soc. Symp. Proc. **36**, 25 (1985).
[28] A. Correia, B. Pichaud, A. Lhorte, and J. B. Quiorin, J. Appl. Phys. **79**, 2145 (1996).
[29] M. Seibt, A. Döller, V. Kveder, A. Sattler, and A. Zozime, phys. stat. sol. (b) **222**, 327 (2000).
[30] S. Solmi and D. Nobili, J. Appl. Phys. **83**, 2484 (1998).
[31] J. Xie and S. P. Chen, Phys. Rev. Lett. **83**, 1795 (1999).
[32] A. Bourret and W. Schröter, Ultramicroscopy **14**, 97 (1984).
[33] J. Utzig, J. Appl. Phys. **64**, 3629 (1986).
[34] R. Kühnapfel and W. Schröter, Mater. Sci. Forum **10–12**, 151 (1986).
[35] For a compilation of data, see: W. Schröter and M. Seibt, in: Properties of Crystalline Silicon, edited by R. Hull (The Institute of Electrical Engineering, London, 1999), p. 543.
[36] W. Shockley and W. T. Read, Phys. Rev. **87**, 835 (1952).
[37] R. N. Hall, Phys. Rev. **87**, 387 (1952).
[38] T. Buonassisi, A. A. Istratov, M. A. Marcus, M. Heuer, M. D. Pickett, B. Lai, Z. Cai, S. M. Heald, and E. R. Weber, Solid State Phenom. **108/109**, 577 (2005).
[39] W. Bergholz, Physica B **116**, 312 (1983).
[40] It should be noted that the temperature has been measured during heating the sample and that gettering processes in this period have been included in the simulations.
[41] E. R. Weber, Appl. Phys. A **30**, 1 (1983).
[42] M. Seibt and W. Schröter, Philos. Mag. A **59**, 337 (1989).

[43] The binary system Si:Au is, similar to Si:Al, a simple eutectic system with a eutectic temperature of 363 °C. Radiotracer experiments have shown that the gettering effect of the Au:Si liquid is even stronger compared to that of Al:Si. In addition, unlike the Al:Si liquids, it is stable even for very long processing times [12, 13].
[44] T. Buonassisi, A. A. Istratov, M. Heuer, M. A. Marcus, R. Jonczyk, J. Isenberg, B. Lai, Z. Cai, S. Heald, W. Warta, R. Schindler, G. Willeke, and E. R. Weber, J. Appl. Phys. **97**, 074901 (2005).
[45] W. Schröter and H. Cerva, Solid State Phenom. **85/86**, 67 (2002).
[46] N. A. Drozdov, A. A. Patrin, and V. D. Tkachev, Sov. Phys. JETP Lett. **23**, 597 (1976).
[47] V. Kveder, M. Badelevych, E. Steinman, A. Izotov, W. Schröter, and M. Seibt, Appl. Phys. Lett. **84**, 2106 (2004).
[48] V. Kveder, M. Badylevich, W. Schröter, M. Seibt, E. Steinman, and A. Izotov, phys. stat. sol. (a) **202**, 901–910 (2005).
[49] W. Schröter, J. Kronewitz, U. Gnauert, F. Riedel, and M. Seibt, Phys. Rev. B **52**, 13726 (1995).
[50] O. Voss, V. V. Kveder, W. Schröter, and M. Seibt, phys. stat. sol. (c) **2**, 1847 (2005).
[51] O. Voss, V. V. Kveder, and M. Seibt, unpublished results.
[52] T. Buonassisi, A. A. Istratov, S. Peters, C. Ballif, J. Isenberg, S. Riepe, W. Warta, R. Schindler, G. Willeke, Z. Cai, B. Lai, and E. R. Weber, Appl. Phys. Lett. **87**, 121918 (2005).
[53] M. Seibt, M. Apel, I. Hanke, and W. Schröter, in: Proceedings of 6th Workshop on the Role of Impurities and Defects in Silicon Device Processing, Snowmass, CO, 11–14 August 1996, p. 118 (NREL/SP-413-21551).
[54] I. Hanke, PhD Thesis, Göttingen 1997 (Cuvillier, Göttingen 1997, ISBN 3-89588-635-1).
[55] S. M. Sze, Physics of Semiconductor Devices (Wiley Interscience, New York, 1981).